Multivariate divergence in wild microbes: no evidence for evolution along a genetic line of least resistance

Emile Gluck-Thaler[1,2*], Muhammad Shaikh[1], Corlett W. Wood[1]

(1) Department of Biology, University of Pennsylvania, Philadelphia, PA, USA

(2) Current address: Department of Plant Pathology, University of Wisconsin-Madison, Madison, WI, USA; Wisconsin Institute for Discovery, Madison, WI, USA

*Corresponding author: gluckthaler@wisc.edu

Abstract

Trait evolution depends both on the direct fitness effects of specific traits and on indirect selection arising from genetically correlated traits. Although well established in plants and animals, the role of trait correlations in microbial evolution remains a major open question. Here, we tested whether genetic correlations in a suite of metabolic traits are conserved between two sister lineages of fungal endophytes, and whether phenotypic divergence between lineages occurred in the direction of the multivariate trait combination containing the most genetic variance within lineages i.e., the genetic lines of least resistance. We found that while one lineage grew faster across nearly all substrates, lineages differed in their mean response to specific substrates and in their overall multivariate metabolic trait means. The structure of the genetic variance-covariance (G) matrix was conserved between lineages, yet to our surprise, divergence in metabolic phenotypes between lineages was nearly orthogonal to the major axis of genetic variation within lineages, indicating that divergence did not occur along the genetic lines of least resistance. Our findings suggest that the evolutionary genetics of trait correlations in microorganisms warrant further research, and highlight the extensive functional variation that exists at very fine taxonomic scales in host-associated microbial communities.

Introduction

Organisms are composed of complex assemblages of correlated traits (Lande and Arnold 1983). Consequently, the evolution of any given trait depends not only on its direct effect on fitness, but also on the indirect effects of the traits with which it is genetically correlated (Wagner 2011). Decades of research in macroorganisms has established that the strength and direction of trait correlations can either constrain or facilitate evolution, depending on their alignment with or opposition to selection, and thereby play a major role in adaptation (Lande 1979; Lande and Arnold 1983; Schluter 1996; Agrawal 2020). In contrast to macroorganisms, it remains unclear whether trait correlations are similarly important in the evolution of microorganisms like bacteria and fungi.

In plants and animals, there is extensive empirical evidence that trait correlations shape evolutionary trajectories within species (Via 1984; Strauss and Irwin 2004; Ingleby et al. 2014; Gompert et al. 2015; McGlothlin et al. 2018; Cope et al. 2021). In short-term selection experiments, this can manifest as a difference between the direction of selection and the direction of the evolutionary response. Over longer evolutionary time, this manifests as divergence among lineages that is aligned with the multivariate trait combination containing the most genetic variance (i.e., the major axis of genetic variation G_{max}) (Schluter 1996). Schluter famously described this pattern as divergence along the "genetic lines of least resistance" (Schluter 1996). Substantial attention has also focused on the evolutionary lability of trait correlations: just like trait means, trait correlations can evolve via the same four evolutionary forces of natural selection, mutation, gene flow, and genetic drift and their

expression is environment dependent (Lande and Arnold 1983; Shaw et al. 1995; Estes and Phillips 2006; Wood and Brodie 2015). There are empirical examples of rapid divergence in trait correlations from artificial selection experiments (Shaw et al. 1995; Steven et al. 2020), as well as between populations (Wood and Brodie 2015). Yet in macroorganisms, the dominant pattern is that trait correlations are surprisingly stable over evolutionary time (Arnold et al. 2008; McGlothlin et al. 2018, 2022).

In microorganisms, however, the evolutionary lability of trait correlations, as well as their impact on the trajectory of evolution remain major open questions. In contrast to macrobes, where several decades of research have investigated evolution through explicitly multivariate frameworks (Lande 1979; Via 1984; Ingleby et al. 2014), a multivariate perspective on trait evolution is much rarer in microbes such as bacteria and fungi (Obeng et al. 2021). There are two major reasons that trait correlations may play a different role in microbial evolution, both related to differences in the modes of inheritance that are common in microbes and macrobes. First, asexual reproduction is more prevalent in microbes than in macrobes. Although relatively few quantitative genetic studies have been performed in asexually reproducing species, existing evidence suggests that genetic covariances differ between sexual and asexual lineages (Nespolo et al. 2008).

Second, horizontal gene transfer is more common in microorganisms like bacteria and fungi (Fitzpatrick 2012; Gluck-Thaler and Slot 2015; Szöllősi et al. 2015; Arnold et al. 2022; Gluck-Thaler et al. 2022; Bucknell and McDonald 2023). As a result, microbial phenotypes are often decoupled from their phylogenetic history such that closely related lineages may not be

84 ecologically similar (Boon et al. 2014; Djemiel et al. 2022). Horizontal gene transfer could
85 restructure correlations between traits if the horizontally transferred genes influence some but
86 not all of the measured traits. Alternatively, if the horizontally transferred genes influence all
87 measured traits, horizontal gene transfer could transport populations to regions of phenotypic
88 space that are not aligned with the major axis of trait correlations. This scenario is plausible if
89 the measured traits are controlled by genes that are typically located close together in microbial
90 genomes, as is often the case for metabolic phenotypes (Wisecaver et al. 2014; Urquhart et al.
91 2023). Taken together, these observations suggest (1) that trait correlations may be more labile
92 in microorganisms than in macroorganisms; and (2) that trait correlations may have a weaker
93 impact on the trajectory of evolution in microorganisms than in macroorganisms.
94
95 The metabolic traits of host-associated microbes are an excellent system in which to test these
96 hypotheses. Host-associated microbes spend much of their lives exposed to complex mixtures
97 of host metabolites (Gershenzon et al. 2012). Consequently, the growth of a host-associated
98 microbe is a multivariate trait that can be decomposed into its ability to metabolize different
99 host substrates (Rokas et al. 2018; Slot and Gluck-Thaler 2019; Westrick et al. 2021). In plants,
100 for example, carbohydrates such as sugars, fibers and starches are often the principal source of
101 carbon accessible to microbes and are growth-promoting resources (Liu et al. 2011). Yet plants
102 also produce secondary metabolites that play multifaceted roles in signalling, growth, and
103 defense (Piasecka et al. 2015). Phenolics, for example, are important constituents of plant cell
104 walls and critical players in constitutive and inducible defense responses against microbial
105 pathogens (Nicholson and Hammerschmidt 1992; López-Goldar et al. 2018; Wallis and
106 Galarneau 2020). As a result, the ability to degrade phenolic compounds is an important

107 determinant of microbial growth on plant tissues (Schäfer et al. 1989; Kliebenstein et al. 2005;
108 Zhao et al. 2019; Nickerson et al. 2023). The simultaneous presence of growth-inhibiting
109 compounds (like secondary metabolites) and growth-promoting compounds (like
110 carbohydrates) suggests that trade-offs between stress tolerance and rapid growth may be an
111 important axis of trait variation in host-associated microorganisms.
112
113 In this study, we compared genetic correlations in a suite of metabolic traits between two
114 lineages of endophytic fungi. We further tested whether divergence in mean metabolic
115 phenotype between lineages occurred along the genetic lines of least resistance (sensu Schluter
116 1996). The endophyte lineages we used in this study are dark septate endophytes, a
117 polyphyletic group of melanized Ascomycete fungi that dominate plant microbiomes across
118 all major plant groups in terrestrial ecosystems (Ruotsalainen et al. 2021). Dark septate
119 endophytes from the Molliciaceae family frequently colonize the roots of *Vaccinium* species,
120 a widely-distributed genus of shrubs that includes blueberry and cranberry (Gorzelak et al.
121 2012; Yang et al. 2018; Morvan et al. 2020). Individual Mollisiaceae species and even
122 individuals within the same species often differ dramatically in their interactions with plants,
123 ranging from commensal to mutualistic to pathogenic (Newsham 2011; Tellenbach et al. 2011;
124 Reininger et al. 2012), suggesting variation within and between species and lineages has
125 important ecological consequences. Yet despite their potential to impact plant host function
126 and their ubiquity, our understanding of phenotypic differences among dark septate endophytes
127 and of the ecological factors shaping their distributions is still in its infancy (Tanney and Seifert
128 2020).
129

130 We isolated two lineages of Molliseaceae endophytes from the roots of lowbush blueberry
131 (*Vaccinium angustifolium*) across three sites in Eastern North America. We then compared
132 endophyte growth across a panel of phenolic and carbohydrate metabolites (to capture their
133 response to specific host chemicals) and extracts of whole plant tissues and organs (to capture
134 their response to more realistic biochemical environments), and tested for differences in trait
135 means and correlations between lineages. We used these two experiments to answer three
136 questions: (1) Have these endophyte lineages diverged in their response to each metabolite and
137 extract, and in their multivariate mean metabolic phenotype? (2) Are there genetic trade-offs
138 between growth on phenolics and carbohydrates, and if so, are these trade-offs conserved
139 across lineages? and (3) Did divergence in mean metabolic phenotypes occur along a genetic
140 line of least resistance (sensu Schluter 1996)?

Materials and Methods

Endophyte and plant material collection

Lowbush blueberry (*V. angustifolium*) plants were sampled from June to October 2020 from three second growth forests in the Eastern United States that are primarily used for scientific research: the research forest at Chatham University's Eden Hall Campus in Richland Township, Pennsylvania (40°39'50.0" N 79°57'12.3" W); Powdermill Nature Reserve in Westmoreland County, Pennsylvania (40°09'41.1" N 79°16'28.9" W); and Mountain Lake Biological Station in Giles County, Virginia (37°22'34.2" N 80°31'12.1" W). At each location, we selected 2-7 sites located at least 500m apart, and within each site we haphazardly sampled 5-10 *V. angustifolium* individuals located at least 10m apart with no observable blueberry plants between them. Fine fibrous roots located no deeper than 10cm from the soil surface were collected from individual plants using a trowel and knife, stored in plastic bags, and used immediately that same day for endophyte isolation.

At Mountain Lake Biological Station in October 2020, we collected additional plant materials to use in the preparation of growth media for two experiments (see below). Whole root systems and attached leaves from approximately 50 *V. angustifolium* plants growing from three large patches were collected on a single day. Root systems and leaves were pooled across sample sites. We also haphazardly collected fallen leaves from *Quercus* spp. (oak) and *Acer* spp. (maple), and fallen needles from a stand of planted *Pinus monticola* (western white pine). Intact plant leaves were collected from the ground and not from living trees to ultimately

164 extract material that Molliseaceae endophytes could be expected to encounter during the
165 saprophytic stage of their lifecycle around the roots of their lowbush blueberry hosts (Tanney
166 and Seifert 2020). Since the leaves were collected from the ground, we were not confident in
167 ID'ing them to the species level. All roots and leaves were kept at -80°C for approximately
168 four months until used for media preparation.
169
170 **Endophyte isolation and genotyping**
171
172 Endophytic fungi were isolated from *V. angustifolium* roots using a sequence of ethanol/bleach
173 sterilization steps followed by direct plating onto 50% strength Modified Melin-Norkrans agar
174 (MMN; Supplementary Methods). A total of 69 fungi isolated from *V. angustifolium* roots with
175 melanized morphologies characteristic of dark septate endophytes were successfully
176 genotyped by sequencing the internal transcribed spacer (ITS) barcoding gene (Table
177 S1)(Gardes and Bruns 1993). We identified each isolate to taxonomic family level using a
178 BLASTn search of their ITS sequence against the NCBI nr/nt database (last accessed
179 01/31/2021). The resulting sample of ITS sequences from Mollisiaceae isolates, along with
180 reference sequences from known species within this family (Tanney and Seifert 2020), were
181 aligned using mafft (--auto)(Katoh and Standley 2013). Pairwise sequence identities between
182 isolates were calculated based on this alignment. Alignments were trimmed using ClipKit
183 (default settings)(Steenwyk et al. 2020), and used to build a maximum likelihood phylogeny
184 with IQtree (-m MFP -b 100) (Nguyen et al. 2015). This phylogeny revealed that 52 isolates
185 could be confidently placed within the Mollisiaceae family.
186

187 Given that species-level classifications are notoriously difficult to resolve in the Mollisiaceae,
188 we used the phylogenetic placements of our isolates relative to the closest described species to
189 provisionally classify them into one of two lineages: the *Phialocephala fortinii* s.l. – *Acephala*
190 *applanata* species complex (PAC) and "Clade D" sensu Tanney and Seifert 2020. PAC
191 contains some of the most well-studied and frequently recovered dark septate endophyte
192 species from coniferous and ericaceous plant roots (Grünig et al. 2008). Clade D is an ad-hoc
193 phylogenetic group which includes *Mollisia nigrescens* and other poorly described root
194 endophytes that have previously been recovered from *Vaccinium* tissues (Tanney and Seifert
195 2020).
196
197 We initially selected $n_{Clade\ D}$ = 13 and n_{PAC} = 17 isolates to phenotype from our available
198 collection by prioritizing isolates with different ITS sequences and/or that were recovered from
199 different host individuals to minimize the phenotyping of clones (Figure 1). While both Clade
200 D and PAC isolates were recovered from the Mountain Lake site ($n_{Clade\ D}$ = 10; n_{PAC} = 14),
201 only Clade D isolates were retained from the Chatham site ($n_{Clade\ D}$ = 3) and only PAC isolates
202 were retained from the Powdermill site (n_{PAC} = 3). We ultimately filtered out several isolates
203 due to quality control issues, resulting in $n_{Clade\ D}$ = 11 for the Metabolite Experiment, $n_{Clade\ D}$ =
204 13 for the Extract Experiment, n_{PAC} = 15 for the Metabolite Experiment and n_{PAC} = 16 for the
205 Extract Experiment (Supplementary Methods) (Parks and Goldman 2014). It is important to
206 note that between 11-16 isolates is on the low end of the sample size used to estimate G-
207 matrices. In a meta-analysis of 95 G-matrices, Wood and Brodie III (2015) found that the
208 median sample size used to estimate a G-matrix was 38.5 families or genotypes (mean = 52.2,
209 range = 5-587). Therefore, while our sample size is within the range of past G-matrix studies,

210 we have relatively limited statistical power to identify small differences in G-matrix structure.
211 In our study, the small number of isolates per lineage is a feature of the challenge of targeting
212 specific microbes for sampling in the field: unlike most macrobes, a microbe's identity cannot
213 be determined without culturing or sequencing it.
214
215 We conducted all statistical analyses described below using isolates from all three sites as well
216 as a more restricted set containing only isolates from Mountain Lake to test whether including
217 isolates from different geographic areas changed our results. Limiting our analysis to Mountain
218 Lake isolates only does not qualitatively change the results of our study. Therefore, we choose
219 to present results from the analysis of isolates from all three sites.
220
221 **Plant metabolite experiment: media preparation and experimental design**
222
223 We compared metabolic trait means and metabolic trait covariances within and between
224 lineages, where we define a metabolic trait as growth on a particular plant-derived substrate.
225 We selected 6 phenolic and 5 carbohydrate metabolites produced across different organs in
226 *Vaccinium* and therefore likely encountered by fungal endophytes colonizing species within
227 this genus (Table S2). We focused on phenolics and carbohydrates to capture potential trade-
228 offs between performance on putatively growth-inhibiting and growth-promoting compounds
229 (however, despite the fact that phenolics are an important component of inducible defenses in
230 plants (Nicholson and Hammerschmidt 1992; López-Goldar et al. 2018; Wallis and Galarneau
231 2020), they did not inhibit growth in our experiment; see Results). We added each metabolite
232 dissolved in ethanol to autoclaved media amended with a hot water extraction of *V.*

233 *angustifolium* roots (Supplementary Methods). Each of the 11 treatments consisted of known
234 physiological concentrations of each metabolite (Stribley and Read 1974; Harris et al. 2007;
235 Riihinen et al. 2008; Kaur et al. 2012; Edwards et al. 2018; Ștefănescu et al. 2020). We used
236 media amended with host root extract to capture the effect that each metabolite may have on
237 endophyte growth in the context of other host-associated metabolites, as opposed to adding
238 metabolites to standardized minimal media. As a control treatment, we added 20ml of pure
239 ethanol to root extract media, for a total of 12 treatments.
240
241 We ran this experiment in three cohorts separated by 1-2 weeks each due to the large number
242 of plates. Each cohort had one replicate of each isolate-metabolite combination (34 isolates x
243 12 treatments = 408 plates / cohort). All plates for a given cohort were prepared on the same
244 day using root extract from one of the six original bags of *V. angustifolium* root system
245 collections (see above) and left to dry for 48 hours in a laminar flow hood. Plates were then
246 inoculated with 4mm plugs from two-week old cultures grown on MMN plates, sealed with
247 micropore tape, haphazardly arranged and incubated upside-down in the dark at room
248 temperature.
249
250 **Plant extract experiment: media preparation and experimental design**
251
252 We selected root and leaf materials from *V. angustifolium,* as well as leaves from three different
253 plant species sympatric with *V. angustifolium* (*Pinus monticola, Quercus* spp. and *Acer* spp.).
254 We used these additional plant species to create ecologically relevant variation in multivariate
255 biochemical environments for the plant extract experiment. In contrast to the metabolite

experiment described above, this experiment was designed to capture potential trade-offs in performance across more realistic biochemical environments. We prepared root and leaf extracts from materials collected at Mountain Lake Biological Station (see above) using a hot water extraction method (Supplementary Methods).

Autoclaved extracts were added to autoclaved DI water agar (15g/L) to a final concentration of 5g/L, and the resulting solutions were immediately poured into plates prepared and left to dry as above. Final extract concentrations in this experiment were 5 times greater than those in the metabolite experiment because they were intended as the main treatment effect. There were 3 replicates per isolate x extract treatment (34 isolates x 5 treatments x 3 replicates = 510 plates), and a single experimental cohort. All plates were prepared on the same day and inoculated and stored as above.

Measuring growth rate

Given that many Mollisiaceae endophytes primarily reproduce through clonal vegetative growth (Tanney and Seifert 2020), growth rates are expected to be important ecological traits (Aguilar-Trigueros et al. 2015). We measured colony area in cm^2 at 7, 14, and 21 days after inoculation and calculated the Area Under the Growth Progress Stairs (AUGPS) as a quantitative measurement of growth over time, such that AUGPS units were cm^2 x 7 days (Supplementary Methods). We calculated AUGPS using the audps function (type = "absolute") in the R package Agricolae (Mendiburu and Simon 2015). While all isolates were able to grow on all treatments, 30 out of the 1,530 plates prepared across all experiments had cultures that

279 did not grow at all over the 21-day period, as occasionally happens during culture-based
280 experiments, and were subsequently discarded. This resulted in at most 1 replicate being
281 discarded for each genotype x treatment combination.
282
283 Haphazardly selected groups of plates were imaged using a vertically mounted Nikon D3500
284 camera equipped with a Nikon AF-P DX 18-55mm f/3.5-5.6G VR lens. A ruler was placed in
285 each image and was used to calibrate measurements. Plates were illuminated from two sides
286 by mounted fluorescent lights. We measured colony area from images of each plate using
287 ImageJ software (Schneider et al. 2012), where the boundaries of each colony were estimated
288 by eye. The colony area at day 0 for all isolates (0.113 cm^2) was determined based on a random
289 sample of 10 plates imaged at this time. Colonies without identifiable boundaries were marked
290 as missing. Images from the extract experiment taken on day 21 were discarded because the
291 media and fungal tissues progressively darkened over this period of time - perhaps due to
292 increased melanization or the activity of secreted enzymes - such that the fungal colony
293 boundaries could not reliably be identified. Growth rates for the Extract Experiment were
294 therefore estimated using two timepoints only, in addition to the starting timepoint at day 0,
295 which limited our ability to capture variation in growth rates between day 14 and 21.
296
297 **Statistical analysis: Linear mixed models**
298
299 Prior to our analyses, we removed 4 isolates originally assigned to Clade D from our dataset
300 due to poor phylogenetic support (Supplementary Methods). In addition, we removed 4 isolates
301 (2 PAC and 2 Clade D) from the metabolite experiment and 1 PAC isolate from the extract

experiment due to possible contamination (Supplementary Methods). We performed all statistical analyses in R 4.1.1 (R Core Team 2016) and unless specified otherwise, created data visualizations using ggplot2 (Wickham et al. 2021). We constructed three different linear mixed models to test for the effects of various predictor variables on isolate growth (i.e., AUGPS) using the "lmer" function in the lme4 package (Bates et al. 2015). We included isolate and isolate-by-treatment interactions as random effects in all models to control for isolate-specific variation.

To test how individual metabolites affected isolate growth in the two endophyte lineages, we constructed a model with metabolite, phylogenetic lineage, metabolite-by-lineage interactions and cohort as fixed effects. To test how chemical class (phenolic or carbohydrate) interacts with lineage membership, we constructed a model with chemical class, phylogenetic lineage, class-by-lineage interactions and cohort as fixed effects and individual metabolite as a random effect to control for metabolite-specific effects independent of chemical class. We fit cohort as a fixed effect rather than a random effect because our experiment included only 3 cohorts, and random-effect variance estimates are imprecise for random effects with fewer than 5-6 levels (Harrison et al. 2018). Finally, to test how plant extracts interact with lineage membership, we constructed a model that included extract treatment phylogenetic lineage and extract-by-lineage interactions as fixed effects.

We tested for the significance of fixed effects with type III sums of squares using the Anova function in the car package (Fox and Weisberg 2011). We confirmed that the residuals within each model met the required assumptions of normality and homoscedasticity by simulating

model residuals using the DHARMa package (Hartig and Lohse 2021) and inspecting the resulting quantile-quantile plot and the plot of the residuals versus the predicted values to detect deviations from the expected distribution. Estimated marginal means and their 95% confidence intervals for each treatment within each lineage were calculated and compared to each other using the emmeans package and post-hoc Tukey tests (Lenth et al. 2021).

Statistical analysis: Comparisons of multivariate G-matrices

To test for differences in the multivariate response to plant chemistry between the two lineages, we calculated and compared the genotypic variance-covariance (**G**) matrices from each lineage for the plant metabolite and plant extract experiments, in addition to carbohydrate- and phenolic-specific G-matrices. In these G-matrices, each isolate trait is its mean-centered growth (AUGPS) averaged across its replicates on a specific metabolite or plant extract. We mean centered AUGPS for each isolate by subtracting the lineage mean from its untransformed AUGPS value, in a process analogous to size correction that is used when comparing different macroorganism species (McGlothlin et al. 2018), in order to increase our power to detect differences in growth due to treatment effect and not differences due to baseline growth rates between lineages. In order to avoid artificially inflating similarity between G-matrices, we removed metabolite treatments from the metabolite experiment that had no statistically significant effect on growth in either lineage (Table S3). This resulted in the removal of two phenolic treatments (chlorogenic acid and vanillic acid) and one carbohydrate treatment (starch). Removal of these treatments do not quantitatively change the results of any multivariate statistical analyses (data not shown). For the metabolite experiment, we averaged

348 growth across cohorts (which were equivalent to experimental replicates) and for the extract
349 experiment, we averaged across replicates. We decomposed each G-matrix into its
350 eigenvectors and eigenvalues using base R's prcomp function (scale = FALSE).
351
352 We calculated three test statistics that capture differences in matrix structure, following
353 previously established methods (Wood and Brodie III 2015): the difference in total genetic
354 variance between endophyte lineages (ΔVt), the difference between the proportion of variance
355 along Gmax (ΔGmax), and the difference in the orientation of Gmax (θ). Gmax represents the
356 largest eigenvector of the covariance matrix and is the linear combination of traits that captures
357 the largest proportion of variation in growth among isolates. A large ΔVt indicates that isolates
358 within one lineage harbor more genetic variation than do isolates in the other lineage. A large
359 ΔGmax indicates that growth on different substrates is more strongly correlated in one lineage
360 than in the other. A large θ indicates that the lineages differ in the direction of trait correlations.
361 To test whether ΔVt, ΔGmax, or θ differed between lineages, we permuted isolates among the
362 two lineage matrices 500 times and recalculated the three test statistics as above from the
363 permuted data to generate null distributions.
364
365 To quantify similarity in overall matrix structure, we calculated correlations between the
366 response to random vectors applied to each lineage's G-matrix using the RandomSkewers
367 function from the evolqg package with 10,000 random gradients (Melo et al. 2016). The
368 random skewers (RS) method applies random vectors of selection gradients to each matrix and
369 measures the correlation between the response vectors of the two matrices. The responses of
370 matrices with similar structures will be highly correlated.

371

372 To examine pairwise correlations between growth on different substrates, we constructed
373 Spearman correlation matrices using base R's cor function. The significance of each
374 correlation coefficient was visualized and calculated using the ggcorplot package (Kassambara
375 2019). Pairwise trait correlations between lineages were compared using the cocor package
376 using the Fisher's z test (Diedenhofen and Musch 2015). *P* values were corrected for multiple
377 comparisons using the Benjamini-Hochberg method implemented in base R's p.adjust
378 function.

379

380 To test for differences in multivariate trait means between lineages, we performed a one-way
381 MANOVA for each experiment where the different substrates were the response variables and
382 lineage was the predictor. Here, we also mean centered trait values by subtracting mean lineage
383 growth across all treatments within a specific experiment from each trait value. This allowed
384 us to remove the overall growth difference between the lineages while preserving the
385 differences between treatments within each lineage. We evaluated the effect size of lineage on
386 substrate using the package effectsize (Ben-Shachar et al. 2020).

387

388 We also used mean centered AUGPS values to calculate Schluter's theta according to the
389 procedure described in Schluter (1996) so we could focus on differences between lineages due
390 to substrate treatment and not basal growth rate (e.g., analogous to using size-corrected species
391 means for animals (McGlothlin et al. 2018)). First, we extracted Gmax from each lineage's G-
392 matrix for each experiment using the prcomp() function in R. Then, we calculated the vector

393 between each lineage's multivariate mean (z), and normalized z such that z'z = 1. Finally, for

394 each lineage, we calculated the angle theta in degrees between its Gmax and z.

395

396 **Results**

397

398 **Lineages differ in baseline growth rates and in their growth on individual plant**
399 **metabolites, chemical classes and plant extracts**

400

401 For the plant metabolite experiment, we found that lineages differed in their baseline growth
402 (lineage effect: $\chi^2_{df=1} = 175.43$, $P < 0.0001$), that metabolites differed in their effects on growth
403 (metabolite effect: $\chi^2_{df=11} = 238.75$, $P < 0.0001$), and that lineages differed in their growth on
404 individual metabolites (lineage-by-metabolite interaction: $\chi^2_{df=11} = 345.16$, $P < 0.0001$)(Figure
405 2; Table S4). The mean growth of the PAC isolates averaged across all treatments and cohorts
406 was significantly greater than the growth of Clade D isolates (LS means: PAC = 64.4 cm^2 x 7
407 days, Clade D = 31.3 cm^2 x 7 days; $P < 0.0001$). In Clade D, growth on rutin, caffeic acid and
408 xylose all differed significantly from the ethanol control media, while in the PAC, all
409 metabolite treatments except chlorogenic acid, vanillic acid and starch differed significantly
410 from the control (Table S5, Figure 2). Treatments with significant effects tended to increase
411 growth, except caffeic acid which negatively affected the PAC (Table S6). The positive effect
412 of caffeic acid on Clade D was such that growth rate differences between the two lineages were
413 abolished when growing on this metabolite after correcting for multiple comparisons (LS
414 means: PAC = 50.7 cm^2 x 7 days, Clade D = 42.9 cm^2 x 7 days; $P_{Bonferroni} = 0.234$). We
415 additionally found a significant effect of experimental cohort ($\chi^2_{df=2} = 126.92$, $P < 0.0001$),
416 indicating that growth rates differed between our experimental cohorts. Differences between
417 treatments were not due to total carbon concentration, as carbon molarity was not significantly

418 correlated with growth in either lineage across all treatments (Pearson's r_{PAC}= 0.01, P_{PAC}=
419 0.83; Pearson's $r_{Clade\ D}$= 0.02, $P_{Clade\ D}$= 0.68; Figure S1).
420
421 We found that lineages differed in their baseline growth across carbohydrate and phenolic
422 chemical classes (lineage effect: $\chi^2_{df=1}$ = 183.38, P < 0.0001) and that lineages differed in their
423 growth on individual chemical classes (lineage by chemical class interaction: $\chi^2_{df=1}$ = 74.50, P
424 < 0.0001; Figure 2B). However, phenolics and carbohydrates alone did not differ in their
425 impact on endophyte growth (chemical effect: $\chi^2_{df=1}$ = 0.35, P = 0.55; Table S7). These main
426 effects were still significant when excluding the caffeic acid treatment (Table S8). The mean
427 growth of PAC isolates was significantly greater than Clade D isolates on both chemical
428 classes (Table S9); however, the magnitude of difference was greater on carbohydrates than
429 on phenolics (LS means for carbohydrates: PAC = 67.7 cm^2 x 7 days, Clade D = 27.8 cm^2 x 7
430 days; LS means for phenolics: PAC = 61.2 cm^2 x 7 days, Clade D = 33.8 cm^2 x 7 days), and
431 remained true when excluding caffeic acid treatments (Table S10). We also found a significant
432 effect of experimental cohort (cohort effect: $\chi^2_{df=2}$ = 32.48, P < 0.0001), indicating that growth
433 rates differed between cohorts.
434
435 For the plant extract experiment, we similarly found that lineages differed in their baseline
436 growth (lineage effect: $\chi^2_{df=1}$ = 542.31, P < 0.0001), that plant extracts differed in their effect
437 on growth (extract effect: $\chi^2_{df=4}$ = 394.12, P < 0.0001), and that lineages responded differently
438 to individual plant extracts (lineage by extract effect: $\chi^2_{df=4}$ = 205.92, P < 0.0001; Table S11,
439 Figure 2). The mean growth of PAC isolates was significantly greater than that of Clade D
440 isolates averaged across all extract types (LS means: PAC = 33.1 cm^2 x 7 days, Clade D = 11

441 cm^2 x 7 days; $P < 0.0001$). Within the PAC, growth on the oak and maple leaf extracts was
442 significantly greater compared with growth on all other extracts, while within Clade D, only
443 the oak leaf treatment was significantly greater compared with all other treatments (Table S12).
444 Although maple and oak are non-host species for these two lineages, maple and oak leaves
445 were abundant at our study sites and may be an important resource during their saprophytic
446 life stage.
447
448 **Lineages differ in their multivariate means across multiple metabolic traits**
449
450 We calculated separate G-matrices for PAC and Clade D for both the metabolite and extract
451 experiments using mean-centered growth data (Methods; Tables S13-20). For the metabolite
452 experiment, the major principal component of the mean-centered G-matrices (PC1, or Gmax)
453 for each lineage captured 73.24% and 54.71% for Clade D and PAC, respectively (Figure 3).
454 Metabolite treatments had similar loadings to each other along each lineage's Gmax,
455 suggesting this axis separates isolates in both lineages according to how fast or slow they grow
456 and independent of any specific treatment. In contrast, treatments differ in their loadings along
457 the second principal component (PC2, capturing 7.77% and 17.42% of variation in growth rate
458 for Clade D and PAC, respectively), which suggests that this axis separates isolates according
459 to metabolite-specific growth responses. We confirmed a significant and large effect of
460 endophyte lineage on mean multivariate metabolite-related growth using a one-way
461 MANOVA (Pillai's trace = 0.93; approximate $F = 67.3$; $df(9,45)$; $P < 0.0001$; Partial eta^2 =
462 0.93). For the plant extract experiment, Gmax captured 84.68% and 72.35% of variation in
463 growth rate and PC2 captured 7.15% and 18.31% for Clade D and PAC, respectively. We

464 observed a significant and large multivariate effect of endophyte lineage on plant extract-
465 related mean growth using a one-way MANOVA (Pillai's trace = 0.87; approximate $F = 101.2$;
466 $df(5,73)$; $P < 0.0001$; Partial eta^2 = 0.87). This indicates that the lineages occupy non-
467 overlapping regions of multivariate metabolic trait space (Figure 3B).
468
469 **Metabolic traits vary with similar strength and in similar directions along the major axis**
470 **of multivariate growth**
471
472 The total genotypic variance of PAC was nearly twice the magnitude of Clade D (200 vs. 110),
473 indicating that there was more variation in growth across metabolites in PAC isolates than
474 Clade D isolates. The difference in total genotypic variance (ΔVt) between the two lineages
475 for the metabolite experiment was significantly greater than expected compared to random
476 chance ($P = 0.02$; Figure 3). Lineages differed marginally in the proportion of variation
477 explained by Gmax (ΔGmax) compared with random expectations ($P = 0.09$), indicating that
478 the strength with which traits covary along Gmax is largely similar among isolates from either
479 lineage. Finally, the difference in the orientation of Gmax (θ) was smaller than expected ($P =$
480 0.05), indicating that within each lineage, the directions in which traits covary are conserved
481 along Gmax.
482
483 The comparisons of Gmax for the metabolite experiment, which provide comparisons along a
484 single dimension of the G-matrix, are in agreement with comparisons of overall G-matrix
485 structure. Random skewers showed that the response to selection predicted from the G-
486 matrices for the two lineages was strongly correlated (random skewers correlation = 0.88, P

487 <0.001). This correlation is not likely not driven by a response to a specific chemical class, as
488 the carbohydrate-specific and phenolic-specific G-matrices were also significantly correlated
489 across the two lineages (random skewers $correlation_{carbohydrates}$ = 0.96, P = 0.005; random
490 skewers $correlation_{phenolics}$ = 0.88, P = 0.025). This indicates that overall, traits vary with similar
491 strength and in similar directions across all dimensions of the G-matrix.
492
493 In contrast for the extract experiment, differences between lineages in total genotypic variance
494 (ΔVt; P = 0.609), the proportion of variation on Gmax (ΔGmax; P = 0.431) and the orientation
495 of Gmax (θ; P = 0.719) did not differ more or less compared to a random expectation. This
496 indicates that PAC isolates are about as different from each other as Clade D isolates when
497 growing on plant extracts and that their traits vary with similar strength and in similar
498 directions (Figure 3). Similar to the metabolite experiment, a random skewers analysis showed
499 that the G-matrices of the two lineages were positively correlated with each other (Random
500 skewers correlation = 0.82, P = 0.026).
501
502 **The strength and direction of pairwise metabolic trait correlations are conserved**
503
504 After comparing the overall multivariate responses of the two lineages, we next compared all
505 pairwise trait correlations between the two lineages to test whether any substrate-specific
506 differences in metabolic trait covariances exist. For the metabolite experiment, all trait
507 correlations tended to be positive within each lineage, with 36/36 showing positive trends in
508 both lineages and with 16/36 of these having positive correlations significantly greater than 0
509 in both lineages (Figure S2). For the extract experiment, all pairwise trait correlations within

510 each lineage were positive, and 4/10 correlations were significantly greater than 0 in both
511 lineages (Figure S2). After correcting for multiple comparisons, we found no evidence that
512 pairwise trait correlations differed between lineages for the metabolite experiment, while only
513 the oak leaf-pine needle trait correlation differed between lineages for the extract experiment
514 (Spearman's $rho_{Clade\ D}$= 0.9, Spearman's rho_{PAC}= 0.2; Fisher's z = -3.01; P = 0.03; Table S21,
515 Figure 4).
516
517 **No evidence for metabolic trait divergence along a genetic line of least resistance**
518
519 We used each lineage's G-matrix, calculated with mean-centered average growth data for each
520 isolate, to test the hypothesis that the metabolism of lineages has diverged along a genetic line
521 of least resistance. In contrast to previous studies that found evidence for morphological
522 divergence along genetic lines of least resistance in multiple animal species (i.e., Schluter's
523 theta = 0) (Schluter 1996; McGlothlin et al. 2018), we found no evidence for metabolic
524 divergence along a line of least resistance between the two endophytic fungal lineages in either
525 the metabolite or extract experiment. Instead, we found that Schluter's theta for PAC relative
526 to Clade D and for Clade D relative to PAC for the metabolite experiment was 81.6° and 86.2°,
527 respectively, and that theta for PAC relative to Clade D and for Clade D relative to PAC for
528 the extract experiment was 91.3° and 83.2°, respectively.
529
530 To provide context to these results, we calculated pairwise nucleotide similarity at the ITS
531 barcode locus between each isolate (Table S22). Mean ITS similarity was 99.6%, 96.8% and
532 87.2% for within PAC, within Clade D and between PAC and Clade D, respectively. A

533 threshold of 88.5% identity at the ITS locus is typical for discriminating between taxonomic
534 families, while species-level thresholds typically range from 97%-100% depending on the
535 fungal taxon in question (Vu et al. 2019).
536

537 **Discussion**

538

539 Here, we found that sister lineages of endophytes isolated from the same host harbor significant
540 genotypic and phenotypic variation related to growth on plant-derived metabolites and
541 extracts. Metabolic trait correlations were broadly conserved between lineages (Figure 3,
542 Figure 4). However, we found no evidence of trade-offs within either lineage between specific
543 carbohydrate and phenolic compounds, perhaps because phenolics did not inhibit endophyte
544 growth, contrary to our initial expectation. However, lineages differed in their relative
545 performance on phenolics versus carbohydrates, indicating that metabolic trade-offs may exist
546 between lineages. Finally, we found that metabolic trait divergence between lineages did not
547 occur along the genetic lines of least resistance. Divergence between the two endophyte
548 lineages was nearly orthogonal to the major axis of genetic variation within lineages. Our
549 results underscore the importance of species-level variation in the microbiome, and suggest
550 that the evolutionary genetics of trait correlations in microorganisms merit further study.

551

552 **Positive correlations between metabolic traits are conserved across lineages**

553

554 A central goal of our study was to test whether trait correlations are conserved across lineages
555 in microorganisms, as they often are in macroorganisms (Arnold et al. 2008). We tested this
556 hypothesis in two complementary experiments that measured endophyte performance across a
557 suite of eleven host-derived metabolites and five plant extracts. In both experiments, we found
558 that correlations between metabolic traits were largely positive and conserved between
559 lineages (Figure 4). Neither the orientation nor magnitude of the major axis of genotypic

560 variation differs between lineages for either metabolite- or extract-related growth phenotypes
561 (Figure 3). Together, the conservation of pairwise positive trait correlations and the major axis
562 of multivariate trait variation suggests that these lineages have maintained a common set of
563 metabolic trait covariances.
564
565 Although we did not detect a difference in the magnitude or direction of genetic correlations
566 between lineages, lineages differed in the total amount of genetic variation (ΔVt) in their
567 response to plant metabolites (Figure 3). The PAC lineage contained almost twice the amount
568 of genetic variation in metabolic traits compared with Clade D. This difference in the amount
569 of standing genetic variation in the metabolic traits implies that our focal lineages differ in
570 their evolutionary capacity to respond to selection imposed by specific metabolites (Roff et al.
571 2012).
572
573 The evolutionary stability of genetic (co)variances is a long-standing question in quantitative
574 genetics (Turelli 1988; Shaw et al. 1995; Arnold et al. 2008; McGlothlin et al. 2022). All four
575 forces of evolution—selection, drift, mutation, and gene flow—can alter genetic variances and
576 reshape covariances between traits (Arnold et al. 2008). Indeed, the G-matrix can evolve
577 rapidly. Selection erodes trait variance (Lande and Arnold 1983; Arnold et al. 2008), and can
578 rapidly alter genetic correlations between traits (Steven et al. 2020). In some cases, **G** differs
579 substantially between populations (Wood and Brodie 2015) and between species (Chakrabarty
580 and Schielzeth 2020). Nevertheless, in many cases the structure of **G** is stable over relatively
581 long timescales (Arnold et al. 2008, McGlothlin et al. 2022) and major environmental clines
582 (Henry and Stinchcombe 2023). Our results are consistent with this latter group of studies,

583 showing that the overall structure of **G** is relatively constant across lineages. We hope that our
584 study will inspire future studies of microbial quantitative genetics, which are necessary to
585 evaluate whether the G-matrix exhibits similar patterns of stability and evolution in micro- and
586 macroorganisms.
587
588 We originally expected that the G-matrices in our study would be dominated by negative
589 genetic covariances between growth on carbohydrates and phenolics. This expectation was
590 based on the fact that sugars, fibers, and starches tend to be easily metabolized by microbes
591 (Liu et al. 2011), while phenolics are involved in plant defense responses against microbial
592 pathogens and tend to inhibit microbial growth (Nicholson and Hammerschmidt 1992; López-
593 Goldar et al. 2018; Wallis and Galarneau 2020). Given the preponderance of stress-related
594 trade-offs across taxa (Ferenci 2016; Züst and Agrawal 2017; He et al. 2022), we hypothesized
595 that performance on growth-inhibiting compounds like phenolics would come at the expense
596 of rapid growth on growth-promoting compounds like carbohydrates. However,we did not
597 observe any statistically significant trade-offs between growth on these different substrates
598 (Figure 4, Figure S2). This may be due to the fact that phenolics were not actually growth-
599 limiting in our experiment (Figure 2A). Both Clade D and PAC grew faster on several different
600 phenolic compounds compared with controls, suggesting that both lineages can use phenolic
601 compounds as a nutrient source. Future studies should examine ecological traits beyond those
602 directly related to the metabolism of plant metabolites, such as abiotic stress tolerance and
603 combative dominance, to test if and how the metabolic traits we measured here are associated
604 with other ecological traits (Bazzaz and Grace 1997; Crowther et al. 2014; Zanne et al. 2020).
605

606 While we did not detect a tradeoff between growth on phenolics and carbohydrates *within*
607 lineages, comparing the lineages to each other revealed some evidence of specialization for
608 different strategies. Clade D tended to have higher growth across all phenolics compared to all
609 carbohydrates, while the opposite was true for PAC (Figure 2B), suggesting that Clade D in is
610 better equipped to assimilate phenolic compounds and PAC is better equipped to assimilate
611 carbohydrates. Indeed, we found a significant lineage x chemical class interaction effect that
612 supports the observation that lineages respond differently to either carbohydrates or phenolics.
613

614 **Lineages diverged in baseline growth rate and in their response to specific metabolites**

615

616 Although trait correlations are largely conserved between the sister lineages of Molliseaceae
617 endophytes in our experiment, they have diverged phenotypically in two major ways. First,
618 they differed in baseline growth rates across nearly all examined metabolites (Figure 2). The
619 differences between lineages in intrinsic growth persisted across the plant extracts, indicating
620 that lineages also differ in growth rate in more complex, ecologically realistic metabolic
621 environments. In addition to differences in baseline growth, lineages differed significantly in
622 their overall multivariate trait means on both metabolite and plant extracts (Figure 3), and in
623 their response to specific substrates, most notably for caffeic acid (Figure 2). Together, the
624 differences in both specific trait means and in the overall multivariate mean suggest the
625 biochemical niches of microbes colonizing the same host are structured by both small
626 differences across multiple traits and by large differences in specific traits.
627

628 Caffeic acid is a common metabolite produced by many plants as a precursor in the production
629 of lignin and is also known to directly inhibit the growth of several bacteria and fungi,
630 suggesting it has potential to act as a defense compound both through strengthening plant cell
631 walls and inhibiting microbial colonization of plant tissues (Ravn et al. 1989; Lanoue et al.
632 2010; Li et al. 2021). The lineage-specific effects we observed for substrates like caffeic acid
633 may arise through several non-mutually exclusive mechanisms. Lineages may differ in their
634 capacity to produce enzymes that detoxify or assimilate the substrate, or may have other
635 compensatory mechanisms for tolerating downstream stresses such as reactive oxygen species
636 (Westrick et al. 2021).
637
638 **Divergence between lineages did not occur along the genetic line of least resistance**
639
640 If trait correlations influence the trajectory of evolution, phenotypic divergence between
641 lineages should be aligned with the multivariate trait combination containing the most genetic
642 variation within lineages (Schluter 1996). Although trait correlations were broadly conserved
643 between the endophyte lineages in our study, to our surprise we found that divergence in the
644 multivariate mean metabolic phenotype was nearly orthogonal to the major axis of genetic
645 variation within lineages. This finding is contrary to studies in macroorganisms over the past
646 two decades that are generally consistent with Schluter's hypothesis (Bégin and Roff 2004;
647 McGuigan et al. 2005; Chenoweth et al. 2010; Bolstad et al. 2014; McGlothlin et al. 2018).
648
649 What might account for this pair of incongruent observations, that trait correlations are
650 conserved between lineages, but that the major axis of genetic variation was not aligned with

651 phenotypic divergence between lineages? One possibility is that our study omitted a major trait
652 or traits that are correlated with the metabolic traits we measured and are under strong selection
653 in wild endophyte populations. Mollisiaceae endophytes are facultative symbionts: they live
654 as endophytes in blueberry roots, but are also capable of functioning as free-living saprotrophs
655 of leaf litter (Tanney and Seifert 2020). Selection can differ dramatically between host-
656 associated and free-living life stages in facultative symbionts (Burghardt et al. 2018). If our
657 experiment omitted an important fitness-related trait from either life stage, indirect selection
658 driven by the missing correlated trait could be responsible for driving evolution orthogonal to
659 the trait correlations we measured, especially if the omitted trait or traits contain extensive
660 genetic variation (Lande and Arnold 1983).
661
662 A second possibility is that the fungal lineages in our experiment are more distantly related
663 than the macroorganisms that have been the predominant focus of past work. Although
664 divergence is expected to follow the genetic line of least resistance over relatively short
665 evolutionary timescales, this pattern may weaken as the divergence time between lineages
666 increases, because **G** itself evolves (Schluter 1996; Arnold et al. 2008; McGlothlin et al. 2018).
667 However, our comparisons of ITS sequences indeed suggest that the fungal lineages in our
668 study are indeed different genera in the same taxonomic family (Tanney and Seifert 2020),
669 similar in taxonomic scope to Schluter's original paper, which included cross-generic
670 comparisons in Galapagos finches and sparrows (Schluter 1996). Furthermore, a recent study
671 in *Anolis* lizards showed that the major axis of genetic divergence shaped phenotypic
672 divergence over relatively long timescales (20-40 million years), even in the face of an
673 evolving G-matrix (McGlothlin et al. 2018).

674

675 Alternatively, horizontal gene transfer could account for divergence in a direction orthogonal
676 to the genetic lines of least resistance. Once thought to be relatively rare in eukaryotes like
677 fungi, the past two decades have revealed extensive evidence for horizontal gene transfer
678 between fungi of genes that confer important ecological functions, including those involved in
679 specialized metabolism (Fitzpatrick 2012; Wisecaver et al. 2014; Gluck-Thaler and Slot 2015;
680 Szöllősi et al. 2015). The pattern we observed—divergence orthogonal to $\mathbf{G}_{\mathbf{max}}$ and little
681 change in **G** itself—could be explained by horizontal transfer of a suite of genes that affect all
682 measured metabolic traits. This could deliver the recipient lineage to a new region of the fitness
683 landscape without altering trait correlations. Mobile genetic elements have previously been
684 implicated in major evolutionary changes via horizontal transfer in bacteria, such as the
685 transfer of antibiotic resistance or the ability to infect a host (Brockhurst et al. 2019; Weisberg
686 and Chang 2023), and large mobile elements carrying metabolic genes and capable of
687 horizontal transfer have recently been discovered in fungi (Vogan et al. 2021; Gluck-Thaler et
688 al. 2022; Urquhart et al. 2022). The impact of horizontally transferable microbial mobile
689 elements on the trajectory of evolution—the direction of evolution in multivariate trait space—
690 in the recipient lineage, merits future research.

691

692 **Future directions: the evolutionary ecology of wild microbes**

693

694 One unique challenge that arises when applying quantitative genetics to wild microbes is that
695 the distinction between *intra*specific and *inter*specific variation is more ambiguous in
696 microorganisms than in macroorganisms (Lücking et al. 2020). The ambiguity that arises when

defining microbial species can complicate the interpretation of G-matrices. If a group of isolates is actually comprised of multiple species, the resulting G-matrix of trait correlations—which will summarize trait variation *among* species—is not a true G-matrix, and may not be a useful predictor of evolutionary trajectories *within* each constituent species. In this study, the endophyte isolates clustered into two well-resolved lineages with a high degree of sequence similarity at the ITS locus within lineages but not between lineages. This is why we considered variation within lineages to reflect intraspecific variation, and differences between lineages to reflect divergence between species. Nevertheless, the ambiguity of what constitutes a true species is a crucial factor to consider when applying quantitative genetics to microbes.

Second, it is often prohibitively difficult to control the number of isolates, lineages, or genera of wild microbes represented in a study *a priori.* It is usually infeasible to strategically target isolates or lineages for field sampling because microbial identity cannot be determined in the field. Instead, identifying wild microbes relies on culture-dependent or -independent methods back in the lab (Su et al. 2012). As a result, the number of isolates, species, or genera included in a study is often outside of the researcher's control, at least relative to taxa that can be reliably identified and targeted for sampling in the field.

An additional complication that arises when estimating genetic (co)variances in clonal species like microbes is that some among-isolate variation may be due to transgenerational plasticity. Transgenerational plasticity is when an individual's phenotype is determined by an environment that its parent (or grandparent or great-grandparent) experienced, rather than the alleles it inherited (Bell and Hellmann 2019). Transgenerational plasticity can inflate genetic

720 (co)variances because it confounds genetic and environmental effects on phenotype.
721 Accounting for this possibility in future microbial experiments requires a system-specific
722 understanding of how rapidly these effects decay in a common garden.
723
724 Finally, the ecological significance of fine-scale taxonomic variation in host-associated
725 microbes merits future research. Our study uncovered significant functional variation among
726 closely related isolates in the same lineage, as well as significant functional divergence
727 between sister lineages. How this variation scales up to influence the structure and function of
728 host-associated communities is a major open question in the field. Through differentially
729 impacting the growth of individual members of the plant microbiome, plant host chemistry
730 may have cascading impacts on endophyte community assembly (Eisenhauer et al. 2017;
731 Clocchiatti et al. 2021). Distinct host chemistries can favor the assembly of distinct endophyte
732 communities (Sietiö et al. 2018; Bonito et al. 2019; Nickerson et al. 2023) and likely shape the
733 distribution of endophyte populations across landscapes through environmental filtering and
734 niche partitioning (Carroll and Petrini 1983; Tedersoo et al. 2013; Wehner et al. 2014; Veach
735 et al. 2019). In turn, differences between endophyte communities may shape variation in plant
736 health outcomes by, for example, influencing interactions with pathogens (Busby et al. 2013),
737 mediating abiotic stress responses (Rodriguez et al. 2008) and promoting or inhibiting plant
738 growth (Alberton et al. 2010; Newsham 2011; Reininger et al. 2012). Further investigations
739 into the evolution of endophyte ecology will thus be critical for dissecting how variation within
740 microbiomes shapes and is in turn shaped by variation in their plant hosts.

741 **Data availability**

742 All supporting data, including raw image files, measurements and R scripts (including alternate
743 scripts for analyzing ML isolates only), are available from the following Figshare repository
744 (https://doi.org/10.6084/m9.figshare.20489715). All sequence data have been deposited at
745 NCBI (GenBank accession numbers OP378573 through OP378602).

746 **Conflict of interest**

747 The authors declare that they have no conflicts of interests.

748 **Acknowledgements**

749 We are grateful for the help of Marion Holmes and Tiffany Betras for getting us to and from
750 our sample sites and providing expert guidance. Thanks to John Wenzel for providing access
751 to the Powdermill Nature Reserve, Jaime Jones for facilitating our sampling at Mountain Lake
752 Biological Station and to Vincent Formica, Chang-Yu Chang, McCall Calvert, Eunnuri Yi and
753 Addison Martin for providing helpful feedback on drafts of this manuscript. This work was
754 supported by startup funds from the University of Pennsylvania to CWW.

755 **Contributions**

756 EGT and CWW conceptualized the research. EGT and MS collected data and EGT conducted
757 formal analyses. EGT wrote the original draft and EGT and CWW participated in reviewing
758 and editing the manuscript.

759

760

761

762 **References**

763 Agrawal, A. A. 2020. A scale-dependent framework for trade-offs, syndromes, and
764 specialization in organismal biology. Ecology 101:e02924.
765 Aguilar-Trigueros, C. A., S. Hempel, J. R. Powell, I. C. Anderson, J. Antonovics, J. Bergmann,
766 T. R. Cavagnaro, et al. 2015. Branching out: Towards a trait-based understanding of fungal
767 ecology. Fungal Biology Reviews 29:34–41.
768 Alberton, O., T. W. Kuyper, and R. C. Summerbell. 2010. Dark septate root endophytic fungi
769 increase growth of Scots pine seedlings under elevated CO2 through enhanced nitrogen use
770 efficiency. Plant and Soil 328:459–470.
771 Arnold, B. J., I.-T. Huang, and W. P. Hanage. 2022. Horizontal gene transfer and adaptive
772 evolution in bacteria. Nature Reviews Microbiology 20:206–218.
773 Arnold, S. J., R. Bürger, P. A. Hohenlohe, B. C. Ajie, and A. G. Jones. 2008. Understanding the
774 Evolution and Stability of the G-Matrix. Evolution 62:2451–2461.
775 Bazzaz, F. A., and J. Grace. 1997. Plant Resource Allocation. Elsevier.
776 Bégin, M., and D. A. Roff. 2004. From Micro- to Macroevolution Through Quantitative Genetic
777 Variation: Positive Evidence from Field Crickets. Evolution 58:2287–2304.
778 Bell, A. M., and J. K. Hellmann. 2019. An Integrative Framework for Understanding the
779 Mechanisms and Multigenerational Consequences of Transgenerational Plasticity. Annual
780 review of ecology, evolution, and systematics 50:97–118.
781 Ben-Shachar, M. S., D. Lüdecke, and D. Makowski. 2020. effectsize: Estimation of Effect Size
782 Indices and Standardized Parameters. Journal of Open Source Software 5:2815.
783 Bolstad, G. H., T. F. Hansen, C. Pélabon, M. Falahati-Anbaran, R. Pérez-Barrales, and W. S.
784 Armbruster. 2014. Genetic constraints predict evolutionary divergence in Dalechampia

785 blossoms. Philosophical Transactions of the Royal Society B: Biological Sciences
786 369:20130255.
787 Bonito, G., G. M. N. Benucci, K. Hameed, D. Weighill, P. Jones, K.-H. Chen, D. Jacobson, et al.
788 2019. Fungal-Bacterial Networks in the Populus Rhizobiome Are Impacted by Soil Properties
789 and Host Genotype. Frontiers in Microbiology 10:481.
790 Boon, E., C. J. Meehan, C. Whidden, D. H.-J. Wong, M. G. Langille, and R. G. Beiko. 2014.
791 Interactions in the microbiome: communities of organisms and communities of genes. Fems
792 Microbiology Reviews 38:90–118.
793 Brockhurst, M. A., E. Harrison, J. P. J. Hall, T. Richards, A. McNally, and C. MacLean. 2019.
794 The Ecology and Evolution of Pangenomes. Current Biology 29:R1094–R1103.
795 Bucknell, A. H., and M. C. McDonald. 2023. That's no moon, it's a Starship: Giant transposons
796 driving fungal horizontal gene transfer. Molecular Microbiology.
797 Burghardt, L. T., B. Epstein, J. Guhlin, M. S. Nelson, M. R. Taylor, N. D. Young, M. J.
798 Sadowsky, et al. 2018. Select and resequence reveals relative fitness of bacteria in symbiotic and
799 free-living environments. Proceedings of the National Academy of Sciences 115:2425–2430.
800 Busby, P. E., N. Zimmerman, D. J. Weston, S. S. Jawdy, J. Houbraken, and G. Newcombe.
801 2013. Leaf endophytes and Populus genotype affect severity of damage from the necrotrophic
802 leaf pathogen, Drepanopeziza populi. Ecosphere 4:art125.
803 Carroll, G., and O. Petrini. 1983. Patterns of Substrate Utilization by Some Fungal Endophytes
804 from Coniferous Foliage. Mycologia 75:53–63.
805 Chakrabarty, A., and H. Schielzeth. 2020. Comparative analysis of the multivariate genetic
806 architecture of morphological traits in three species of Gomphocerine grasshoppers. Heredity
807 124:367–382.

808 Chenoweth, S. F., H. D. Rundle, and M. W. Blows. 2010. The Contribution of Selection and
809 Genetic Constraints to Phenotypic Divergence. The American Naturalist 175:186–196.
810 Clocchiatti, A., S. E. Hannula, M. van den Berg, M. P. J. Hundscheid, and W. de Boer. 2021.
811 Evaluation of Phenolic Root Exudates as Stimulants of Saptrophic Fungi in the Rhizosphere.
812 Frontiers in Microbiology 12.
813 Cope, O. L., K. Keefover-Ring, E. L. Kruger, and R. L. Lindroth. 2021. Growth–defense trade-
814 offs shape population genetic composition in an iconic forest tree species. Proceedings of the
815 National Academy of Sciences 118:e2103162118.
816 Crowther, T. W., D. S. Maynard, T. R. Crowther, J. Peccia, J. R. Smith, and M. A. Bradford.
817 2014. Untangling the fungal niche: the trait-based approach. Frontiers in Microbiology 5.
818 Diedenhofen, B., and J. Musch. 2015. cocor: A Comprehensive Solution for the Statistical
819 Comparison of Correlations. PLoS ONE 10:e0121945.
820 Djemiel, C., P.-A. Maron, S. Terrat, S. Dequiedt, A. Cottin, and L. Ranjard. 2022. Inferring
821 microbiota functions from taxonomic genes: a review. GigaScience 11:giab090.
822 Edwards, K. R., E. Kaštovská, J. Borovec, H. Šantrůčková, and T. Picek. 2018. Species effects
823 and seasonal trends on plant efflux quantity and quality in a spruce swamp forest. Plant and Soil
824 426:179–196.
825 Eisenhauer, N., A. Lanoue, T. Strecker, S. Scheu, K. Steinauer, M. P. Thakur, and L. Mommer.
826 2017. Root biomass and exudates link plant diversity with soil bacterial and fungal biomass.
827 Scientific Reports 7:44641.
828 Estes, S., and P. C. Phillips. 2006. Variation in pleiotropy and the mutational underpinnings of
829 the G-matrix. Evolution 60:2655–2660.
830 Ferenci, T. 2016. Trade-off Mechanisms Shaping the Diversity of Bacteria. Trends in

831 Microbiology 24:209–223.

832 Fitzpatrick, D. A. 2012. Horizontal gene transfer in fungi. FEMS microbiology letters 329:1–8.

833 Gershenzon, J., A. Fontana, M. Burow, U. Wittstock, and J. Degenhardt. 2012. Mixtures of plant
834 secondary metabolites: metabolic origins and ecological benefits. Pages 56–77 *in* G. R. Iason, M.
835 Dicke, and S. E. Hartley, eds. The Ecology of Plant Secondary Metabolites: From Genes to
836 Global Processes, Ecological Reviews. Cambridge University Press, Cambridge.

837 Gluck-Thaler, E., T. Ralston, Z. Konkel, C. G. Ocampos, V. D. Ganeshan, A. E. Dorrance, T. L.
838 Niblack, et al. 2022. Giant Starship Elements Mobilize Accessory Genes in Fungal Genomes.
839 Molecular Biology and Evolution 39:msac109.

840 Gluck-Thaler, E., and J. C. Slot. 2015. Dimensions of Horizontal Gene Transfer in Eukaryotic
841 Microbial Pathogens. PLOS Pathogens 11:e1005156.

842 Gompert, Z., J. P. Jahner, C. F. Scholl, J. S. Wilson, L. K. Lucas, V. Soria-Carrasco, J. A.
843 Fordyce, et al. 2015. The evolution of novel host use is unlikely to be constrained by trade-offs
844 or a lack of genetic variation. Molecular Ecology 24:2777–2793.

845 Gorzelak, M. A., S. Hambleton, and H. B. Massicotte. 2012. Community structure of ericoid
846 mycorrhizas and root-associated fungi of Vaccinium membranaceum across an elevation
847 gradient in the Canadian Rocky Mountains. Fungal Ecology, Fungi and Global Change 5:36–45.

848 Hadacek, F., and G. F. Kraus. 2002. Plant root carbohydrates affect growth behaviour of
849 endophytic microfungi. FEMS microbiology ecology 41:161–170.

850 Harris, C. S., A. J. Burt, A. Saleem, P. M. Le, L. C. Martineau, P. S. Haddad, S. A. L. Bennett, et
851 al. 2007. A single HPLC-PAD-APCI/MS method for the quantitative comparison of phenolic
852 compounds found in leaf, stem, root and fruit extracts of Vaccinium angustifolium.
853 Phytochemical Analysis 18:161–169.

854 Harrison, X. A., L. Donaldson, M. E. Correa-Cano, J. Evans, D. N. Fisher, C. E. D. Goodwin, B.
855 S. Robinson, et al. 2018. A brief introduction to mixed effects modelling and multi-model
856 inference in ecology. PeerJ 6:e4794.
857 He, Z., S. Webster, and S. Y. He. 2022. Growth–defense trade-offs in plants. Current Biology
858 32:R634–R639.
859 Henry, G. A., and J. R. Stinchcombe. 2023. G-matrix stability in clinally diverging populations
860 of an annual weed. Evolution 77:49–62.
861 Ho, A., D. P. Di Lonardo, and P. L. E. Bodelier. 2017. Revisiting life strategy concepts in
862 environmental microbial ecology. FEMS microbiology ecology 93.
863 Ingleby, F. C., D. J. Hosken, K. Flowers, M. F. Hawkes, S. M. Lane, J. Rapkin, C. M. House, et
864 al. 2014. Environmental heterogeneity, multivariate sexual selection and genetic constraints on
865 cuticular hydrocarbons in Drosophila simulans. Journal of Evolutionary Biology 27:700–713.
866 Katoh, K., and D. M. Standley. 2013. MAFFT Multiple Sequence Alignment Software Version
867 7: Improvements in Performance and Usability. Molecular Biology and Evolution 30:772–780.
868 Kaur, J., D. Percival, L. J. Hainstock, and J.-P. Privé. 2012. Seasonal growth dynamics and
869 carbon allocation of the wild blueberry plant (Vaccinium angustifolium Ait.). Canadian Journal
870 of Plant Science 92:1145–1154.
871 Kliebenstein, D. J., H. C. Rowe, and K. J. Denby. 2005. Secondary metabolites influence
872 Arabidopsis/Botrytis interactions: variation in host production and pathogen sensitivity. The
873 Plant Journal 44:25–36.
874 Lande, R. 1979. Quantitative Genetic Analysis of Multivariate Evolution, Applied to Brain:
875 Body Size Allometry. Evolution 33:402–416.
876 Lande, R., and S. J. Arnold. 1983. The Measurement of Selection on Correlated Characters.

877 Evolution 37:1210–1226.
878 Lanoue, A., V. Burlat, G. J. Henkes, I. Koch, U. Schurr, and U. S. R. Röse. 2010. De novo
879 biosynthesis of defense root exudates in response to Fusarium attack in barley. The New
880 Phytologist 185:577–588.
881 Li, S., J. Pi, H. Zhu, L. Yang, X. Zhang, and W. Ding. 2021. Caffeic Acid in Tobacco Root
882 Exudate Defends Tobacco Plants From Infection by Ralstonia solanacearum. Frontiers in Plant
883 Science 12.
884 Liu, Q., A. J. Parsons, H. Xue, K. Fraser, G. D. Ryan, J. A. Newman, and S. Rasmussen. 2011.
885 Competition between foliar Neotyphodium lolii endophytes and mycorrhizal Glomus spp. fungi
886 in Lolium perenne depends on resource supply and host carbohydrate content. Functional
887 Ecology 25:910–920.
888 López-Goldar, X., C. Villari, P. Bonello, A. K. Borg-Karlson, D. Grivet, R. Zas, and L.
889 Sampedro. 2018. Inducibility of Plant Secondary Metabolites in the Stem Predicts Genetic
890 Variation in Resistance Against a Key Insect Herbivore in Maritime Pine. Frontiers in Plant
891 Science 9.
892 Lücking, R., M. C. Aime, B. Robbertse, A. N. Miller, H. A. Ariyawansa, T. Aoki, G. Cardinali,
893 et al. 2020. Unambiguous identification of fungi: where do we stand and how accurate and
894 precise is fungal DNA barcoding? IMA Fungus 11:14.
895 McGlothlin, J. W., M. E. Kobiela, H. V. Wright, J. J. Kolbe, J. B. Losos, and E. D. Brodie. 2022.
896 Conservation and Convergence of Genetic Architecture in the Adaptive Radiation of Anolis
897 Lizards. The American Naturalist 200:E207–E220.
898 McGlothlin, J. W., M. E. Kobiela, H. V. Wright, D. L. Mahler, J. J. Kolbe, J. B. Losos, and E. D.
899 Brodie. 2018. Adaptive radiation along a deeply conserved genetic line of least resistance in

Anolis lizards. Evolution Letters 2:310–322.

McGuigan, K., S. F. Chenoweth, M. W. Blows, and A. E. J. M. Cheverud. 2005. Phenotypic Divergence along Lines of Genetic Variance. The American Naturalist 165:32–43.

Morvan, S., H. Meglouli, A. Lounès-Hadj Sahraoui, and M. Hijri. 2020. Into the wild blueberry (Vaccinium angustifolium) rhizosphere microbiota. Environmental Microbiology 22:3803–3822.

Nespolo, R. F., C. C. Figueroa, M. Plantegenest, and J. C. Simon. 2008. Short-term population differences in the genetic architecture of life history traits related to sexuality in an aphid species. Heredity 100:374–381.

Newsham, K. K. 2011. A meta-analysis of plant responses to dark septate root endophytes. New Phytologist 190:783–793.

Nguyen, L.-T., H. A. Schmidt, A. von Haeseler, and B. Q. Minh. 2015. IQ-TREE: A Fast and Effective Stochastic Algorithm for Estimating Maximum-Likelihood Phylogenies. Molecular Biology and Evolution 32:268–274.

Nicholson, R. L., and R. Hammerschmidt. 1992. Phenolic Compounds and Their Role in Disease Resistance. Annual Review of Phytopathology 30:369–389.

Nickerson, M. N., L. P. Moore, and J. M. U'Ren. 2023. The impact of polyphenolic compounds on the in vitro growth of oak-associated foliar endophytic and saprotrophic fungi. Fungal Ecology 62:101226.

Obeng, N., F. Bansept, M. Sieber, A. Traulsen, and H. Schulenburg. 2021. Evolution of Microbiota-Host Associations: The Microbe's Perspective. Trends in Microbiology 29:779–787.

Parks, S. L., and N. Goldman. 2014. Maximum Likelihood Inference of Small Trees in the Presence of Long Branches. Systematic Biology 63:798–811.

Piasecka, A., N. Jedrzejczak-Rey, and P. Bednarek. 2015. Secondary metabolites in plant innate

923 immunity: conserved function of divergent chemicals. New Phytologist 206:948–964.
924 Rasmussen, S., A. J. Parsons, S. Bassett, M. J. Christensen, D. E. Hume, L. J. Johnson, R. D.
925 Johnson, et al. 2007. High nitrogen supply and carbohydrate content reduce fungal endophyte
926 and alkaloid concentration in Lolium perenne. New Phytologist 173:787–797.
927 Ravn, H., C. Andary, G. Kovács, and P. Mølgaard. 1989. Caffeic acid esters as in vitro inhibitors
928 of plant pathogenic bacteria and fungi. Biochemical Systematics and Ecology 17:175–184.
929 Reininger, V., C. R. Grünig, and T. N. Sieber. 2012. Host species and strain combination
930 determine growth reduction of spruce and birch seedlings colonized by root-associated dark
931 septate endophytes. Environmental Microbiology 14:1064–1076.
932 Riihinen, K., L. Jaakola, S. Kärenlampi, and A. Hohtola. 2008. Organ-specific distribution of
933 phenolic compounds in bilberry (Vaccinium myrtillus) and "northblue" blueberry (Vaccinium
934 corymbosum x V. angustifolium). Food Chemistry 110:156–160.
935 Rodriguez, R. J., J. Henson, E. Van Volkenburgh, M. Hoy, L. Wright, F. Beckwith, Y.-O. Kim,
936 et al. 2008. Stress tolerance in plants via habitat-adapted symbiosis. The ISME journal 2:404–
937 416.
938 Roff, D. A., J. M. Prokkola, I. Krams, and M. J. Rantala. 2012. There is more than one way to
939 skin a G matrix. Journal of Evolutionary Biology 25:1113–1126.
940 Rokas, A., J. H. Wisecaver, and A. L. Lind. 2018. The birth, evolution and death of metabolic
941 gene clusters in fungi. Nature Reviews Microbiology 16:731–744.
942 Ruotsalainen, A. L., M. Kauppinen, P. R. Wäli, K. Saikkonen, M. Helander, and J. Tuomi. 2021.
943 Dark septate endophytes: mutualism from by-products? Trends in Plant Science 0.
944 Schäfer, W., D. Straney, L. Ciuffetti, H. D. Van Etten, and O. C. Yoder. 1989. One Enzyme
945 Makes a Fungal Pathogen, But Not a Saprophyte, Virulent on a New Host Plant. Science

946 246:247–249.
947 Schluter, D. 1996. Adaptive Radiation Along Genetic Lines of Least Resistance. Evolution
948 50:1766–1774.
949 Schneider, C. A., W. S. Rasband, and K. W. Eliceiri. 2012. NIH Image to ImageJ: 25 years of
950 image analysis. Nature Methods 9:671–675.
951 Shaw, F. H., R. G. Shaw, G. S. Wilkinson, and M. Turelli. 1995. Changes in Genetic Variances
952 and Covariances: G Whiz! Evolution 49:1260–1267.
953 Sietiö, O.-M., T. Tuomivirta, M. Santalahti, H. Kiheri, S. Timonen, H. Sun, H. Fritze, et al. 2018.
954 Ericoid plant species and Pinus sylvestris shape fungal communities in their roots and
955 surrounding soil. New Phytologist 218:738–751.
956 Slot, J. C., and E. Gluck-Thaler. 2019. Metabolic gene clusters, fungal diversity, and the
957 generation of accessory functions. Current Opinion in Genetics & Development, Evolutionary
958 genetics 58–59:17–24.
959 Steenwyk, J. L., T. J. B. Iii, Y. Li, X.-X. Shen, and A. Rokas. 2020. ClipKIT: A multiple
960 sequence alignment trimming software for accurate phylogenomic inference. PLOS Biology
961 18:e3001007.
962 Ștefănescu, B.-E., L. F. Călinoiu, F. Ranga, F. Fetea, A. Mocan, D. C. Vodnar, and G. Crișan.
963 2020. The Chemical and Biological Profiles of Leaves from Commercial Blueberry Varieties.
964 Plants 9:1193.
965 Steven, J. C., I. A. Anderson, E. D. Brodie III, and L. F. Delph. 2020. Rapid reversal of a
966 potentially constraining genetic covariance between leaf and flower traits in Silene latifolia.
967 Ecology and Evolution 10:569–578.
968 Strauss, S. Y., and R. E. Irwin. 2004. Ecological and Evolutionary Consequences of Multispecies

969 Plant-Animal Interactions. Annual Review of Ecology, Evolution, and Systematics 35:435–466.
970 Stribley, D. P., and D. J. Read. 1974. The Biology of Mycorrhiza in the Ericaceae. New
971 Phytologist 73:731–741.
972 Su, C., L. Lei, Y. Duan, K.-Q. Zhang, and J. Yang. 2012. Culture-independent methods for
973 studying environmental microorganisms: methods, application, and perspective. Applied
974 Microbiology and Biotechnology 93:993–1003.
975 Sun, K., F.-M. Zhang, N. Kang, J.-H. Gong, W. Zhang, Y. Chen, and C.-C. Dai. 2019. Rice
976 carbohydrate dynamics regulate endophytic colonization of Diaporthe liquidambaris in response
977 to external nitrogen. Fungal Ecology 39:213–224.
978 Szöllősi, G. J., A. A. Davín, E. Tannier, V. Daubin, and B. Boussau. 2015. Genome-scale
979 phylogenetic analysis finds extensive gene transfer among fungi. Philosophical Transactions of
980 the Royal Society of London. Series B, Biological Sciences 370:20140335.
981 Tanney, J. B., and K. A. Seifert. 2020. Mollisiaceae: An overlooked lineage of diverse
982 endophytes. Studies in Mycology 95:293–380.
983 Tedersoo, L., M. Mett, T. A. Ishida, and M. Bahram. 2013. Phylogenetic relationships among
984 host plants explain differences in fungal species richness and community composition in
985 ectomycorrhizal symbiosis. The New Phytologist 199:822–831.
986 Tellenbach, C., C. R. Grünig, and T. N. Sieber. 2011. Negative effects on survival and
987 performance of Norway spruce seedlings colonized by dark septate root endophytes are primarily
988 isolate-dependent. Environmental Microbiology 13:2508–2517.
989 Turelli, M. 1988. Phenotypic Evolution, Constant Covariances, and the Maintenance of Additive
990 Variance. Evolution 42:1342–1347.
991 Urquhart, A. S., N. F. Chong, Y. Yang, and A. Idnurm. 2022. A large transposable element

992 mediates metal resistance in the fungus Paecilomyces variotii. Current Biology 32:937-950.e5.
993 Urquhart, A. S., A. A. Vogan, D. M. Gardiner, and A. Idnurm. 2023. Starships are active
994 eukaryotic transposable elements mobilized by a new family of tyrosine recombinases.
995 Proceedings of the National Academy of Sciences of the United States of America
996 120:e2214521120.
997 Veach, A. M., R. Morris, D. Z. Yip, Z. K. Yang, N. L. Engle, M. A. Cregger, T. J. Tschaplinski,
998 et al. 2019. Rhizosphere microbiomes diverge among Populus trichocarpa plant-host genotypes
999 and chemotypes, but it depends on soil origin. Microbiome 7:76.
1000 Via, S. 1984. The Quantitative Genetics of Polyphagy in an Insect Herbivore. II. Genetic
1001 Correlations in Larval Performance Within and Among Host Plants. Evolution 38:896–905.
1002 Vogan, A. A., S. L. Ament-Velásquez, E. Bastiaans, O. Wallerman, S. J. Saupe, A. Suh, and H.
1003 Johannesson. 2021. The Enterprise, a massive transposon carrying Spok meiotic drive genes.
1004 Genome Research.
1005 Vu, D., M. Groenewald, M. de Vries, T. Gehrmann, B. Stielow, U. Eberhardt, A. Al-Hatmi, et al.
1006 2019. Large-scale generation and analysis of filamentous fungal DNA barcodes boosts coverage
1007 for kingdom fungi and reveals thresholds for fungal species and higher taxon delimitation.
1008 Studies in Mycology 92:135–154.
1009 Wagner, A. 2011. Genotype networks shed light on evolutionary constraints. Trends in Ecology
1010 & Evolution 26:577–584.
1011 Wallis, C. M., and E. R.-A. Galarneau. 2020. Phenolic Compound Induction in Plant-Microbe
1012 and Plant-Insect Interactions: A Meta-Analysis. Frontiers in Plant Science 11.
1013 Wehner, J., J. R. Powell, L. A. H. Muller, T. Caruso, S. D. Veresoglou, S. Hempel, and M. C.
1014 Rillig. 2014. Determinants of root-associated fungal communities within Asteraceae in a semi-

1015 arid grassland. Journal of Ecology 102:425–436.
1016 Weisberg, A. J., and J. H. Chang. 2023. Mobile Genetic Element Flexibility as an Underlying
1017 Principle to Bacterial Evolution. Annual Review of Microbiology 77:null.
1018 Westrick, N. M., D. L. Smith, and M. Kabbage. 2021. Disarming the Host: Detoxification of
1019 Plant Defense Compounds During Fungal Necrotrophy. Frontiers in Plant Science 12.
1020 Wisecaver, J. H., J. C. Slot, and A. Rokas. 2014. The Evolution of Fungal Metabolic Pathways.
1021 PLOS Genetics 10:e1004816.
1022 Wood, C. W., and E. D. Brodie III. 2015. Environmental effects on the structure of the G-matrix.
1023 Evolution 69:2927–2940.
1024 Yang, H., X. Zhao, C. Liu, L. Bai, M. Zhao, and L. Li. 2018. Diversity and characteristics of
1025 colonization of root-associated fungi of Vaccinium uliginosum. Scientific Reports 8:15283.
1026 Zanne, A. E., K. Abarenkov, M. E. Afkhami, C. A. Aguilar-Trigueros, S. Bates, J. M. Bhatnagar,
1027 P. E. Busby, et al. 2020. Fungal functional ecology: bringing a trait-based approach to plant-
1028 associated fungi. Biological Reviews 95:409–433.
1029 Zhao, T., D. Kandasamy, P. Krokene, J. Chen, J. Gershenzon, and A. Hammerbacher. 2019.
1030 Fungal associates of the tree-killing bark beetle, Ips typographus, vary in virulence, ability to
1031 degrade conifer phenolics and influence bark beetle tunneling behavior. Fungal Ecology, From
1032 antagonism to mutualism: the chemical basis of insect-fungus interactions 38:71–79.
1033 Züst, T., and A. A. Agrawal. 2017. Trade-Offs Between Plant Growth and Defense Against
1034 Insect Herbivory: An Emerging Mechanistic Synthesis. Annual Review of Plant Biology
1035 68:513–534.
1036
1037

1038 **Figure legends**

1039 **Figure 1: Two lineages of Mollisiacean endophytes sampled from wild *Vaccinium***
1040 ***angustifolium* roots across multiple sites in Eastern North America.** A) A maximum
1041 likelihood phylogeny of the ITS sequences of all Mollisiacean fungi isolated as part of this
1042 study and reference sequences obtained from public databases. Isolates from this study are
1043 highlighted in green if part of the *Phialocephala fortinii* s.l. – *Acephala applanata* species
1044 complex (PAC), highlighted in orange if part of the ad-hoc phylogenetic group Clade D, and
1045 reference sequences are not highlighted. Bootstrap support is labeled in red and all branches
1046 with <70% bootstrap support have been collapsed. B) Pictures of typical Clade D (left) and
1047 PAC (right) isolates after two weeks growth on 1% blueberry root extract media C)
1048 Approximate locations of sample sites in Pennsylvania (PA) and Virginia (VA), with the
1049 proportion of each lineage from each site visualized as a pie chart.

1050

1051 **Figure 2: Endophyte lineages differ in their intrinsic growth rates and respond**
1052 **differently to specific plant metabolites, metabolite classes, and plant extracts.** Dot plots
1053 displaying fungal growth (cm^2 x 7 days), as measured by the Area Under the Growth Progress
1054 Stairs (AUGPS), in response to A) metabolite treatments, B) metabolite class and C) plant
1055 extracts. Estimated marginal means were calculated separately for the PAC and Clade D
1056 lineages and are overlaid as a large circle on top of individual data points that represent all
1057 cohorts and replicates of each isolate for each treatment. Individual data points are color coded
1058 by lineage, while treatment means that differ significantly from the control (panel A; $\alpha = 0.05$)
1059 or from the blueberry root extract treatment (panel C; $\alpha = 0.05$) are color coded by lineage and

1060 otherwise have a white fill if not significant. Error bars represent the 95% confidence interval,
1061 and points are arranged to be non-overlapping with jitter = 0.02.
1062
1063 **Figure 3: Metabolic trait architecture is largely conserved between endophyte lineages.**
1064 Top: scaled biplots where the X and Y axes represent the first two principal components of the
1065 phenotypic variance/covariance (**P**) matrix for mean-centered metabolic traits in the PAC and
1066 Clade D endophyte lineages for A and B) the metabolite experiment and C and D) the extract
1067 experiment. Individual points represent individual isolates. Loadings for individual
1068 metabolites or plant extracts along PC1/Gmax and PC2 are drawn as black arrows and labeled
1069 in red. Bottom: Null distributions and observed values for the three matrix comparison
1070 statistics (difference in total phenotypic variance, difference in percent variance along
1071 PC1/Gmax and difference in the orientation of PC1/Gmax) for E) the metabolite experiment
1072 and F) the extract experiment. Null distributions were calculated by permuting isolates among
1073 lineages and comparing the features of 500 randomly permuted matrix pairs.
1074
1075 **Figure 4: The vast majority of pairwise metabolic trait correlations do not differ between**
1076 **endophyte lineages.** Each cell in these two matrices contains a *P* value associated with the
1077 null hypothesis that the pairwise trait correlation does not differ between the PAC and Clade
1078 D lineages for A) metabolite experiment and B) extract experiment. Statistical comparisons of
1079 Spearman's rank correlation coefficients were conducted using the Fisher's *z* test.

1080 **Supplementary Information Legends**

1081

1082 **Figure S1:** The linear association between carbon concentration and growth across all
1083 metabolite treatments and fungal lineages

1084

1085 **Figure S2:** Spearman's rho correlations between growth across a) metabolite treatments and
1086 b) plant extract treatments for the PAC and Clade D fungal lineages. Non-significant
1087 correlations ($P > 0.05$) are crossed out.

1088

1089 **Table S1:** Fungal isolate ITS genotyping and best BLASTn hit from NCBI nr

1090

1091 **Table S2:** Carbohydrate and Phenolic metabolites known to be produced by Vaccinium
1092 species

1093

1094 **Table S3:** Metabolite treatments with no statistically discernible effect on the growth of either
1095 PAC or Clade D lineages

1096

1097 **Table S4:** Analysis of Deviance Table of the linear model with individual metabolite
1098 treatments as fixed effects for the metabolite experiment (Type III Wald $\chi 2$ tests)

1099

1100 **Table S5:** Estimated marginal means comparisons of all treatments vs. ethanol control in PAC
1101 and cladeD

1102

1103 **Table S6:** Estimated marginal means comparisons between PAC and cladeD for each
1104 metabolite treatment
1105
1106 **Table S7:** Analysis of Deviance Table of the linear model with carbohydrate and phenolic
1107 chemical class as fixed effects for the metabolite experiment (Type III Wald $\chi 2$ tests)
1108
1109 **Table S8:** Anova of fixed effects in model for phenolics vs carbohydrates, excluding caffeic
1110 acid
1111
1112 **Table S9:** Estimated marginal means comparisons between PAC and cladeD for carbohydrates
1113 and phenolics
1114
1115 **Table S10:** Estimated marginal means comparisons between PAC and cladeD for
1116 carbohydrates and phenolics, excluding caffeic acid
1117
1118 **Table S11:** Analysis of Deviance Table of the linear model with plant extract treatments as
1119 fixed effects for the extract experiment (Type III Wald $\chi 2$ tests)
1120
1121 **Table S12:** Estimated marginal means comparisons of all plant extract treatments in PAC and
1122 cladeD
1123
1124 **Table S13:** G-matrix for mean isolate AUGPS (Clade D, metabolite experiment, n = 11
1125 isolates)

1126

1127 **Table S14:** Eigenvalues and eigenvectors of the G-matrix for mean isolate AUGPS (Clade D,
1128 metabolite experiment, n = 11 isolates)

1129

1130 **Table S15:** G-matrix for mean isolate AUGPS (PAC, metabolite experiment, n = 15 isolates)

1131

1132 **Table S16:** Eigenvalues and eigenvectors of the G-matrix for mean isolate AUGPS (PAC,
1133 metabolite experiment, n = 15 isolates)

1134

1135 **Table S17:** G-matrix for mean isolate AUGPS (Clade D, extract experiment, n = 13 isolates)

1136

1137 **Table S18:** Eigenvalues and eigenvectors of the G-matrix for mean isolate AUGPS (Clade D,
1138 extract experiment, n = 13 isolates)

1139

1140 **Table S19:** G-matrix for mean isolate AUGPS (PAC, extract experiment, n = 16 isolates)

1141

1142 **Table S20:** Eigenvalues and eigenvectors of the G-matrix for mean isolate AUGPS (PAC,
1143 extract experiment, n = 16 isolates)

1144

1145 **Table S21:** Tests for differences between the pairwise trait correlations of cladeD and PAC
1146 for both the metabolite and extract experiment

1147

1148 **Table S22:** Pairwise nucleotide identity at the ITS locus across all isolates

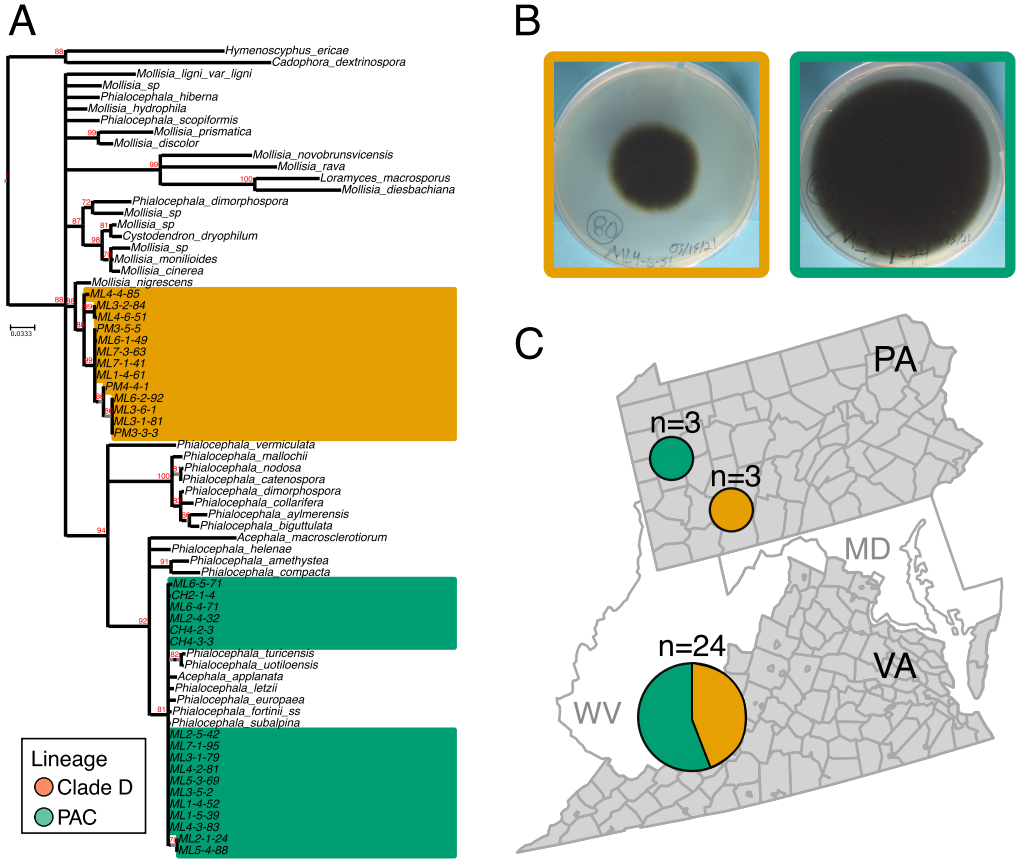
A
Hymenoscyphus_ericae
Cadophora_dextrinospora
Mollisia_ligni_var_ligni
Mollisia_sp
Phialocephala_hiberna
Mollisia_hydrophila
Phialocephala_scopiformis
Mollisia_prismatica
Mollisia_discolor
Mollisia_novobrunsvicensis
Mollisia_rava
Loramyces_macrosporus
Mollisia_diesbachiana
Phialocephala_dimorphospora
Mollisia_sp
Mollisia_sp
Cystodendron_dryophilum
Mollisia_sp
Mollisia_monilioides
Mollisia_cinerea
Mollisia_nigrescens
ML4-4-85
ML3-2-84
ML4-6-51
PM3-5-5
ML6-1-49
ML7-3-63
ML7-1-41
ML1-4-61
PM4-4-1
ML6-2-92
ML3-6-1
ML3-1-81
PM3-3-3
Phialocephala_vermiculata
Phialocephala_mallochii
Phialocephala_nodosa
Phialocephala_catenospora
Phialocephala_dimorphospora
Phialocephala_collariferа
Phialocephala_aylmerensis
Phialocephala_biguttulata
Acephala_macrosclerotiorum
Phialocephala_helenae
Phialocephala_amethystea
Phialocephala_compacta
ML6-5-71
CH2-1-4
ML6-4-71
ML2-4-32
CH4-2-3
CH4-3-3
Phialocephala_turicensis
Phialocephala_uotiloensis
Acephala_applanata
Phialocephala_letzii
Phialocephala_europaea
Phialocephala_fortinii_ss
Phialocephala_subalpina
ML2-5-42
ML7-1-95
ML3-1-79
ML4-2-81
ML5-3-69
ML3-5-2
ML1-4-52
ML1-5-39
ML4-3-83
ML2-1-24
ML5-4-88
0.0333
Lineage
Clade D
PAC
B
C
PA
n=3
n=3
MD
n=24
VA
WV

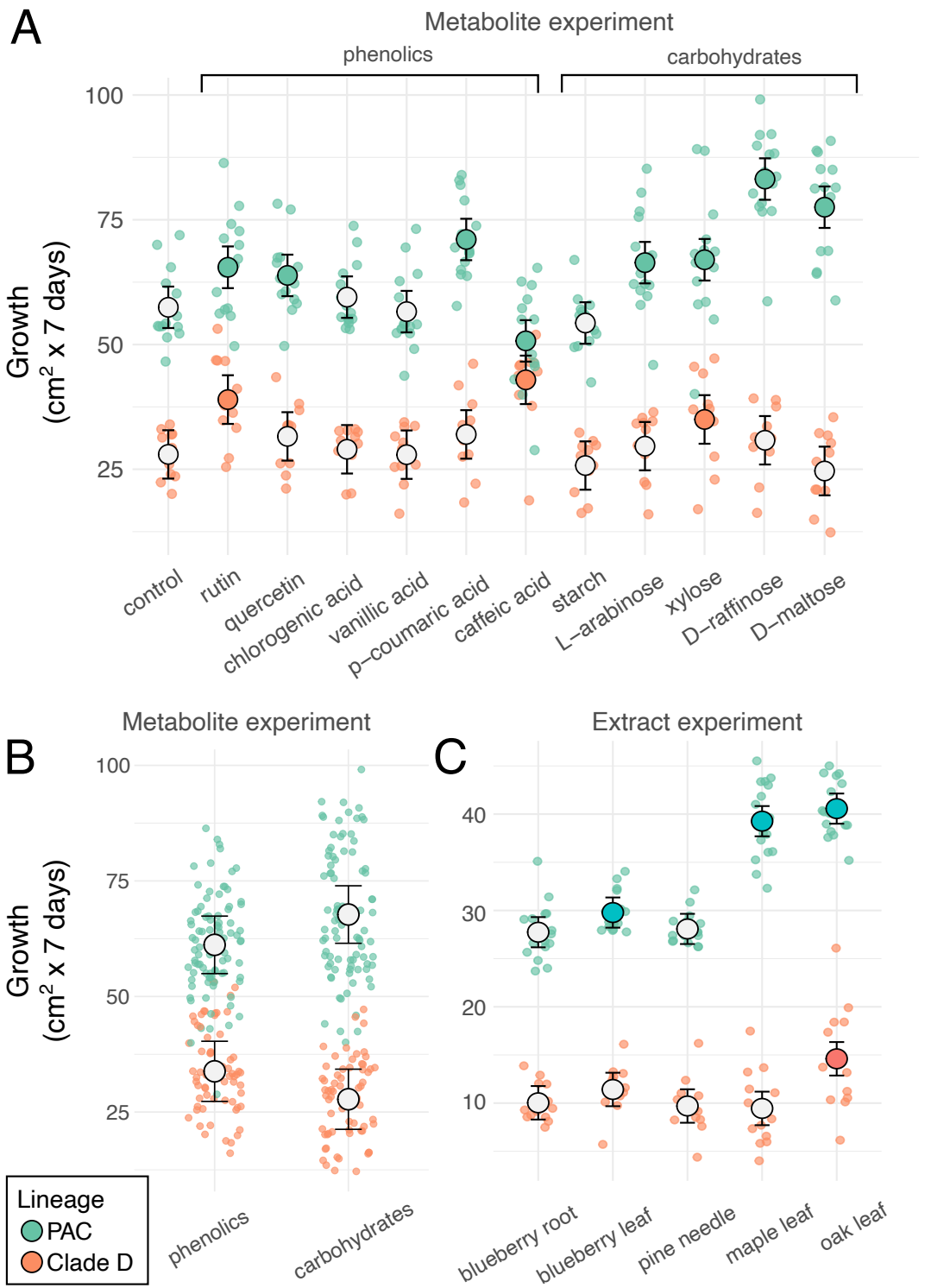
A
Metabolite experiment
phenolics
carbohydrates
Growth
(cm2 x 7 days)
100
75
50
25
control
rutin
quercetin
chlorogenic acid
vanillic acid
p–coumaric acid
caffeic acid
starch
L–arabinose
xylose
D–raffinose
D–maltose
B
Metabolite experiment
Growth
(cm2 x 7 days)
100
75
50
25
phenolics
carbohydrates
C
Extract experiment
40
30
20
10
blueberry root
blueberry leaf
pine needle
maple leaf
oak leaf
Lineage
PAC
Clade D

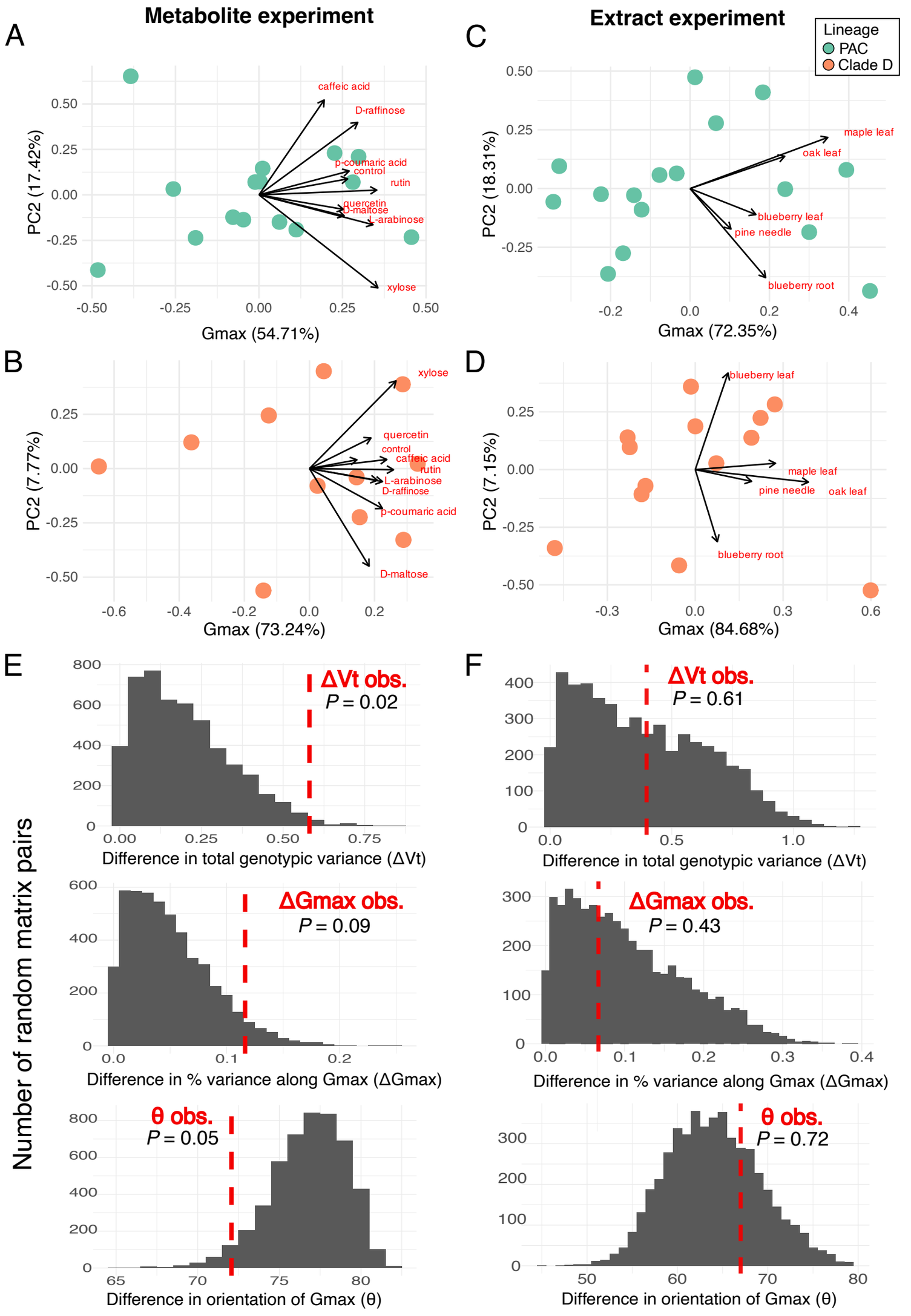
A
Metabolite experiment
caffeic acid
D-raffinose
p-coumaric acid
control
rutin
quercetin
D-maltose
L-arabinose
xylose
PC2 (17.42%)
Gmax (54.71%)
B
xylose
quercetin
control
caffeic acid
rutin
L-arabinose
D-raffinose
p-coumaric acid
D-maltose
PC2 (7.77%)
Gmax (73.24%)
C
Extract experiment
Lineage
PAC
Clade D
maple leaf
oak leaf
blueberry leaf
pine needle
blueberry root
PC2 (18.31%)
Gmax (72.35%)
D
blueberry leaf
maple leaf
pine needle
oak leaf
blueberry root
PC2 (7.15%)
Gmax (84.68%)
E
ΔVt obs.
P = 0.02
Difference in total genotypic variance (ΔVt)
ΔGmax obs.
P = 0.09
Difference in % variance along Gmax (ΔGmax)
θ obs.
P = 0.05
Difference in orientation of Gmax (θ)
F
ΔVt obs.
P = 0.61
Difference in total genotypic variance (ΔVt)
ΔGmax obs.
P = 0.43
Difference in % variance along Gmax (ΔGmax)
θ obs.
P = 0.72
Difference in orientation of Gmax (θ)
Number of random matrix pairs

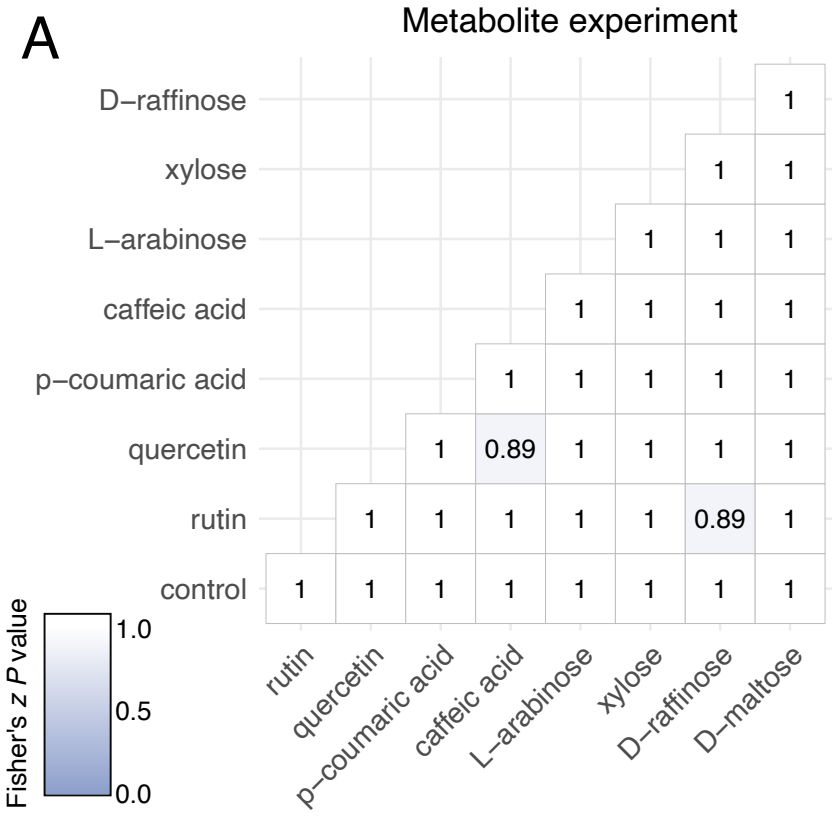
A
Metabolite experiment
D−raffinose
xylose
L−arabinose
caffeic acid
p−coumaric acid
quercetin
rutin
control
rutin
quercetin
p−coumaric acid
caffeic acid
L−arabinose
xylose
D−raffinose
D−maltose
Fisher's z P value
1.0
0.5
0.0

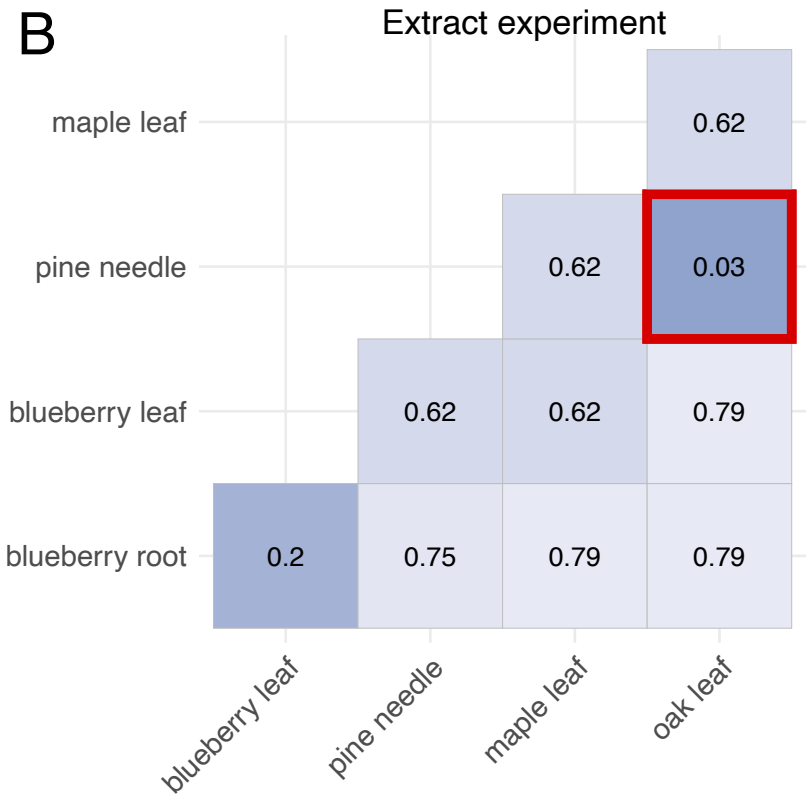
B
Extract experiment
maple leaf
pine needle
blueberry leaf
blueberry root
blueberry leaf
pine needle
maple leaf
oak leaf